



Article

The Problems of Passive Remote Sensing of the Earth's Surface in the Range of 1.2–1.6 GHz

Gennady V. Golubkov ^{1,2}, Mikhail I. Manzhelii ³, Alexandr A. Berlin ¹, Lev V. Eppelbaum ⁴ , Alexey A. Lushnikov ⁵, Igor I. Morozov ¹, Alexey V. Dmitriev ^{6,7} , Sergey O. Adamson ¹, Yuri A. Dyakov ¹, Andrey N. Morozov ⁸ and Maxim G. Golubkov ^{1,*}

- ¹ Semenov Federal Research Center for Chemical Physics, Russian Academy of Sciences, 119991 Moscow, Russia; kolupanovo@gmail.com (G.V.G.); berlin@chph.ras.ru (A.A.B.); morozov@center.chph.ras.ru (I.I.M.); sergey.o.adamson@gmail.com (S.O.A.); yuri_dyakov@mail.ru (Y.A.D.)
- ² National Research Center "Kurchatov Institute", 123182 Moscow, Russia
- ³ Center for Chemical Physics of Atmosphere, 119991 Moscow, Russia; mike.manzhelii@gmail.com
- ⁴ Department of Earth Sciences, Tel Aviv University, Tel Aviv 69978, Israel; levap@tauex.tau.ac.il
- ⁵ Geophysical Center, Russian Academy of Sciences, 119296 Moscow, Russia; Alex.Lushnikov@mail.ru
- ⁶ Institute of Space Science and Engineering, National Central University, Jhongli 32001, Taiwan; dalexav@mail.ru
- ⁷ Skobeltsyn Institute of Nuclear Physics, Lomonosov Moscow State University, 119991 Moscow, Russia
- ⁸ Bauman Moscow State Technical University, 105005 Moscow, Russia; amor59@mail.ru
- * Correspondence: golubkov@chph.ras.ru; Tel.: +7-495-9397322

Received: 14 April 2020; Accepted: 16 June 2020; Published: 18 June 2020



Abstract: The main problems of remote sensing of the Earth's surface within the frequency range 1.2–1.6 GHz are discussed. They are related to the resonant quantum properties of the radio wave propagation medium in the lower ionosphere. It is shown that, for the passive remote sensing, the main source is incoherent microwave radiation of the D and E ionospheric layers in the decimeter range. For the first time, a theoretically grounded principally new scheme of measurements is suggested. The scheme assumes that the radiation source exists below the satellite orbit and accounts for the fact that two types of radiation (direct and reflected) reach the satellite sensor. The separation of the respective fluxes is a serious problem that should be solved for the correct interpretation of the measurements. The question is raised regarding the correct calibration of measuring equipment, depending on the current state of the ionosphere.

Keywords: remote sensing of Earth's surface; D and E ionospheric layers; charged aerosols; equipment calibration

1. Introduction

Currently, considerable interest is given to the physicochemical processes, with the participation of electronically excited states taking place in the lower ionosphere of the Earth, which is primarily associated with the problems of remote passive location of the Earth's surface [1–3]. A spontaneous increase in solar activity accompanied by a significant increase in electromagnetic radiation leads to noticeable perturbations of the propagation medium. These disturbances at altitudes of 60–110 km give rise to the failures of the global navigation satellite systems (GNSS), operating in the frequency range of 1.2–1.6 GHz [4,5].

This paper outlines the possible solutions of existing problems of remote sensing of the Earth's surface. These problems are shown to be closely related to each other. The spectral properties of incoherent microwave radiation from nonequilibrium plasma in the E and D layers of the ionosphere located at heights of 80–110 km (below the orbiting satellites) are considered. This radiation is shown to

be the main source for the passive remote sensing at a frequency of 1.4 GHz. A radical overhaul of the general measurement scheme is proposed and the necessary technical conditions for its implementation are developed. In conclusion, the issue of the correct calibration of measuring equipment was raised.

2. Passive Remote Sensing. State of Art

It was shown [6–8] that, at altitudes from 60 to 110 km, the Sun flares produce a super background ultra high frequency UHF radiation with intensity hundreds of times higher the typical levels of microwave solar bursts. An analysis of the different mechanisms of generation of the detected radiation showed that the largest contribution to the resulting spectrum picture comes from the transitions between Rydberg states of the neutral components of a non-equilibrium two-temperature plasma excited by fluxes of sunlight and slow electrons penetrating in the low ionosphere [1–4]. Incoherent UHF radiation from Rydberg states during geomagnetic disturbances is accompanied earlier by an intense long-wave infrared (IR) radiation (with the wavelength exceeding 15 μm) [9]. The analysis of the spectrum of this radiation allows for restoring the parameters of the two-temperature plasma (electron concentration and temperature) by solving the respective inverse problem [3].

Passive remote sensing involves the use of natural radiation to determine the properties of the Earth's surface, which is usually carried out with receivers operating at a frequency of 1.4 GHz, since, at this frequency, there is a single-parameter dependence of the signal power on the electron concentration [3]. There is still no unique physical understanding among specialists regarding the source of radiation at a frequency of 1.4 GHz [2]. It was previously assumed that this source has a cosmic origin and it corresponds to the radiation of a hydrogen line with a wavelength of 21 cm and a transition frequency $\nu = 1.4204$ GHz, corresponding to an energy of $5.86 \cdot 10^{-6}$ eV [10].

This line is the most important in the interstellar luminescence and corresponds to the forbidden transition between sublevels of the hyperfine structure of the $1^2S_{1/2}$ ground electronic state of the hydrogen atom. The upper sublevel corresponds to the parallel arrangement of the spins of the electron and proton, and the lower corresponds to the antiparallel one. The probability of transition between them is equal $2.85 \cdot 10^{-15} \text{s}^{-1}$ (i.e., one transition is carried out in 11 million years). It is believed that the intensity of radio emission according to the Rayleigh–Jeans law is proportional to temperature, i.e., in a rather narrow spectral range the kinetic temperature of the gas can serve as a measure of the radiation intensity [11,12].

Estimates show that, as a result of resonance rescattering of hydrogen radio emission on Rydberg states in the D and E layers of the Earth's ionosphere for normal geomagnetic conditions and electron concentration $n_e = 10^4 \text{ cm}^{-3}$ at the altitude of 110 km, the power of the cosmic radiation flux arriving at the radiometer is 10^{-32} W/cm^2 [13]. The flux density of intrinsic incoherent UHF radiation of the low ionosphere is about 10^{-25} W/cm^2 [14]. The aforesaid is also confirmed by the fact that direct measurements with a radiometer under normal conditions showed that the maximum effect is only achieved in the daytime, when the microwave radiation is caused by the action of the Sun [15].

A large number of original articles, reviews, and monographs are devoted to the remote sensing of the Earth's surface (see, for example, the lists of publications in [1,2]). However, these publications do not take the delay in the propagation distortion of radio waves as a result of resonant scattering during the passage of D and E layers of the ionosphere at an altitude of 60–110 km into account [7]. In addition, they do not take into account both a direct super background microwave radiation coming to the satellite from the D and E layers of ionosphere and the signal attenuation due to the interaction with charged aerosol layers [1–3].

Before discussing various types of passive remote sensing, we begin with its generally accepted definition. Measuring or obtaining information regarding some properties of an object or phenomenon using a "recording device" without physical contact with the object or phenomenon being studied is referred by the American Society of Photogrammetry and Remote Sensing (ASPRS) to as the *passive remote sensing*. A recording device is a sensor that is mounted on a satellite in space or in an airplane in the troposphere, as well as directly above the surface of the Earth.

Recent developments in the field of technology for passive remote sensing of the Earth’s surface have demonstrated increased interest in the possibility of determining the soil moisture from space. It was found that these measurements are most conveniently carried out in the decimeter range at a frequency of 1.4 GHz [16]. However, errors eventually arise during measurements, the physical cause of which is not yet clear despite of insistent attempts.

To this end, the model approaches has been developed together with various types of experimental methods of sounding. For example, the authors of one of these approaches have suggested that the main source of error in restoring the soil moisture has come neglecting the Faraday effect (polarization of reflected radiation) [17]. On the other hand, the experiment [18] has directly confirmed that the radiation at a frequency of 1.4 GHz has propagated without a significant interaction with the atmosphere, and no polarization has been observed. At the same time, the authors of this work suggested that radiation reflected from grass or leaf cover wetted by rain might be partially polarized. Because, as indicated above, the radiation sources from the D and E layers of the ionosphere are not coherent [7], there is no sense to discuss the influence of the Faraday effect. In fact, during quadrature decomposition of a non-monochromatic signal in the receiver band near the frequency of 1.4 GHz, such a rotation of the polarization vector and a change in its modulus should be observed that is completely determined by the dynamic state of the atmosphere [7]. At the same time, when analyzing the data in the framework of the SMOS (Soil Moisture and Ocean Salinity) program, a significant difference was found between the readings of sensors installed on an airplane at an altitude of 3 km and sensors that are located above the Earth’s surface at an altitude of 150 m [19]. This fact also did not find an explanation in current literature. Generally speaking, in the case of equilibrium radiation, the readings of sensors installed at any altitude (e.g., on airplane and near the Earth’s surface) should coincide, but this is not observed. Therefore, the assumption that the incident radiation is equilibrium is not fair and the approach developed in [20,21] is not applicable.

Next assuming that the sources of incoherent microwave radiation are located inside the D and E layers of the ionosphere, we consider one of a possible schemes measurement when the satellite and aircraft are located vertically along the z axis (for this purpose, generally speaking, it is convenient to use an airship). We also assume that the satellite and the airship are at altitudes H_s and H_a , respectively (see Figure 1), we introduce the time-averaged radiation flux powers at a frequency of 1.4 GHz, as calculated by the «Rydberg» program [6,7,14] independently without taking into account interfering factors. The respective fluxes are marked by a bar above. This is a direct upward radiation $\bar{I}_{\text{tot}}^{(z\uparrow)}(H_s)$ coming to the satellite from the D and E layers and a direct downward radiation $\bar{I}_{\text{tot}}^{(z\downarrow)}(H_a)$ coming from these layers to the airship from above, and the total power of the radiation flux $\bar{I}_{\text{tot}}^{(z\downarrow)}(H_E)$ incident on the surface of the Earth. Subsequently, the measured powers of the incident and reflected radiation fluxes are given by simple expressions:

$$I_{\text{in}}^{(z\downarrow)}(H_E) = \bar{I}_{\text{tot}}^{(z\downarrow)}(H_E)(1 - f), \tag{1}$$

$$I_{\text{in}}^{(z\downarrow)}(H_a) = \bar{I}_{\text{tot}}^{(z\downarrow)}(H_a)(1 - f_1), \tag{2}$$

$$I_{\text{ref}}^{(z\uparrow)}(H_a) = I_{\text{ref}}^{(z\uparrow)}(H_E)(1 - f_2), \tag{3}$$

$$I_{\text{ref}}^{(z\uparrow)}(H_s) = \bar{I}_{\text{tot}}^{(z\uparrow)}(H_s) + I_{\text{ref}}^{(z\uparrow)}(H_E)(1 - f). \tag{4}$$

Here, $f = f_1 + f_2$ is a complete attenuation factor of the power flow of incoherent microwave radiation intensity due to the influence of layers of charged aerosols. The value f_1 is the attenuation of the power of the stream on its way from the D layer to the airship at altitude H_a , f_2 is the attenuation of the flux propagating from the airship to the surface of the Earth (planetary boundary layer). We now

introduce the reflection coefficient $k_r(H_E) = I_{\text{ref}}^{(z\uparrow)}(H_E)/I_{\text{in}}^{(z\downarrow)}(H_E)$ and the following quantities that were directly measured by the sensors,

$$\eta_{aE} = I_{\text{ref}}^{(z\uparrow)}(H_a)/I_{\text{ref}}^{(z\uparrow)}(H_E), \Delta(H_E) = I_{\text{in}}^{(z\downarrow)}(H_E) - I_{\text{ref}}^{(z\uparrow)}(H_E),$$

and define the reflected radiation coming from the Earth's surface as

$$\Delta(H_s) = I_{\text{ref}}^{(z\uparrow)}(H_E)(1 - f) = I_{\text{ref}}^{(z\uparrow)}(H_s) - \bar{I}_{\text{tot}}^{(z\uparrow)}(H_s). \tag{5}$$

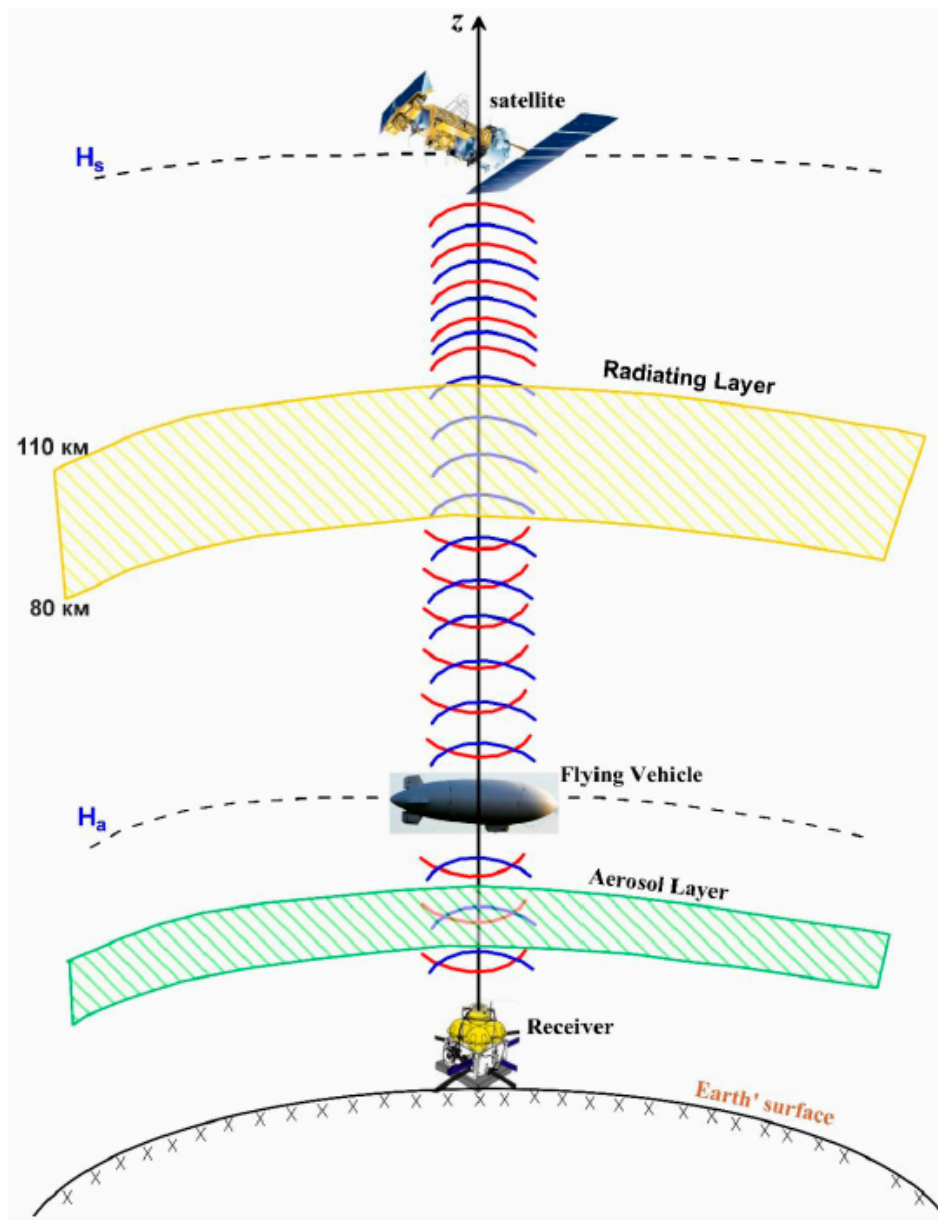


Figure 1. The scheme of measurements by the method of passive remote sensing. Yellow indicates the radiating layer and green indicates the charged aerosol layer. Red lines along the vertical axis are direct radiation up and down from the D and E ionospheric layers; blue lines are radiation reflected from the Earth's surface. Dotted lines H_s and H_a set the trajectory of the satellite and airship.

Equations (1)–(4), yield the following useful relationships:

$$\Delta(H_s) = \frac{\Delta(H_E)k_r(H_E)(1 - f)}{1 - k_r(H_E)}, \tag{6}$$

$$f_1 = \eta_{aE} - \frac{[1 - k_r(H_E)]\Delta(H_s)}{k_r(H_E)\Delta(H_E)}, \quad f_2 = 1 - \eta_{aE} \tag{7}$$

The advantage of Equations (5)–(7) is that the right-hand sides of these expressions are expressed via the relative values of the parameters that were measured by the sensors and independently calculated power of the additional stream $\bar{I}_{\text{tot}}^{(z\uparrow)}(H_s)$. We also note that, in the case of a slight decrease in the incident UHF radiation above the airship, when $f_1 \rightarrow 0$ and the factor $f \rightarrow 1 - \eta$, denoting the power of the reflected radiation coming to the satellite (4) become equal

$$\Delta(H_s) = \frac{\Delta(H_E)k_r(H_E)\eta_{aE}}{1 - k_r(H_E)}. \tag{8}$$

Expression (8) is conveniently used in the analysis of the role of acidic industrial emissions in the planetary boundary layer, starting from several hundred meters.

The obvious question comes up as to what kind of information can be obtained if measurements on the Earth surface are excluded in the general scheme, i.e., express the values k_r , f_1 and f_2 through the averaged power fluxes at atmospheric altitudes H_s and H_a , respectively. Because, by definition $I_{\text{in}}^{(z\downarrow)}(H_E) = \bar{I}_{\text{tot}}^{(z\downarrow)}(H_E)(1 - f)$, then, while using Equations (1)–(4), for the reflection coefficient and attenuation factors, we can derive the following simple expressions:

$$k_r(H_E) = \frac{\Delta(H_s)}{(1 - f)^2 \bar{I}_{\text{tot}}^{(z\downarrow)}(H_E)}, \tag{9}$$

$$f_1 = 1 - \frac{I_{\text{in}}^{(z\downarrow)}(H_a)}{\bar{I}_{\text{tot}}^{(z\downarrow)}(H_a)}, \tag{10}$$

$$f_2 = 1 - I_{\text{in}}^{(z\downarrow)}(H_a) \frac{(1 - k_r(H_E))\Delta(H_s)}{k_r(H_E)}, \tag{11}$$

which, as in the case of “full” experiment, include the values of $\bar{I}_{\text{tot}}^{(z\downarrow)}(H_E)$ and $\bar{I}_{\text{tot}}^{(z\downarrow)}(H_a)$, calculated using the “Rydberg” program [6]. The use of Equations (9)–(11) is of interest for carrying out the synchronous vertical scanning along a portion of the Earth’s surface simultaneously from a satellite and an airship. Moreover, the joint use of Equations (7) and (10) can decrease the measurement errors.

As a result of multiple rescattering on Rydberg complexes in the D and E layers of the ionosphere, the phase of the signal arriving at the receiver is random and, thus, should be characterized by a distributed value. Therefore, increasing the accuracy of measurements by recording the phase of the received signal is not informative.

2.1. Aircraft Measurements

No less useful for remote sensing is the case that describes the situation when we restrict ourselves to using one aircraft, without resorting to satellite measurements. Subsequently, using Equations (1)–(3), the attenuation coefficients of the radiation f_1 and f_2 , the power of the reflected $I_{\text{ref}}^{(z\uparrow)}(H_E)$ and incident $I_{\text{in}}^{(z\downarrow)}(H_E)$ fluxes, and the reflection coefficient $k_r(H_E)$ can be cast into the form:

$$f_2 = \left(\frac{I_{\text{in}}^{(z\downarrow)}(H_a)}{\bar{I}_{\text{tot}}^{(z\downarrow)}(H_a)} \right) \cdot \alpha_{aE}, \tag{12}$$

$$I_{\text{ref}}^{(z\uparrow)}(H_E) = I_{\text{ref}}^{(z\uparrow)}(H_a) \cdot \left(\frac{\bar{I}_{\text{tot}}^{(z\downarrow)}(H_a)}{\bar{I}_{\text{tot}}^{(z\downarrow)}(H_E)} \right) \cdot \alpha_{aE}, \tag{13}$$

$$I_{\text{in}}^{(z\downarrow)}(H_E) = \bar{I}_{\text{tot}}^{(z\downarrow)}(H_E) \cdot \left(\frac{I_{\text{in}}^{(z\downarrow)}(H_a)}{\bar{I}_{\text{tot}}^{(z\downarrow)}(H_a)} \right) \cdot \beta_{aE}, \tag{14}$$

$$k_r(H_E) \equiv \frac{I_{\text{ref}}^{(z\uparrow)}(H_E)}{I_{\text{in}}^{(z\downarrow)}(H_E)} = \frac{I_{\text{ref}}^{(z\uparrow)}(H_a)}{I_{\text{in}}^{(z\downarrow)}(H_a)} \cdot \left(\frac{\bar{I}_{\text{tot}}^{(z\downarrow)}(H_a)}{\bar{I}_{\text{tot}}^{(z\downarrow)}(H_E)} \right)^2 \cdot \beta_{aE}^2, \tag{15}$$

where Equation (10) defines f_1 , and the factors α and β are equal to

$$\alpha_{aE} = \frac{\bar{I}_{\text{tot}}^{(z\downarrow)}(H_E) - \bar{I}_{\text{tot}}^{(z\downarrow)}(H_a)}{\bar{I}_{\text{tot}}^{(z\downarrow)}(H_E) - I_{\text{in}}^{(z\downarrow)}(H_a)}, \beta_{aE} = \frac{\bar{I}_{\text{tot}}^{(z\downarrow)}(H_a) - I_{\text{in}}^{(z\downarrow)}(H_a)}{\bar{I}_{\text{tot}}^{(z\downarrow)}(H_E) - I_{\text{in}}^{(z\downarrow)}(H_a)}.$$

It is seen that the values from Equations (12)–(15) can be completely determined on the aircraft from the measured powers of the incident $I_{\text{in}}^{(z\downarrow)}(H_a)$ and incoming (reflected from the surface), radiation fluxes, and the calculated data obtained using the “Rydberg” program. In other words, a combined version of the measurements is realized here.

2.2. Satellite Passive Remote Sensing

The final limiting case corresponds to the simultaneous exclusion of measurements on the surface of the Earth and the aircraft. Subsequently, only Equation (10) connecting k_r and f remains for analyzing the results. This approach is uninformative. The only way out of this situation (and, strictly speaking, fundamentally wrong) is the vanishing of the quantity f leading to equality $I_{\text{in}}^{(z\downarrow)}(H_E) = \bar{I}_{\text{tot}}^{(z\downarrow)}(H_E)$. It is this case that corresponds to the current level of passive remote sensing, where, as noted above, there is no single point of view on the source of radiation $I_{\text{in}}^{(z\downarrow)}(H_E)$ coming to the surface [1].

The authors of the SMOS project use radiometric sounding, where the main information parameter is the brightness temperature, i.e., they virtually use simple ideas about blackbody radiation, in order to analyze soil moisture from a satellite [22]. The value measured on the satellite $\bar{I}_{\text{tot}}^{(z\uparrow)}(H_s)$ is actually the sum of two radiations: the direct incoherent one from D and E layers and reflected from the surface (see (4)). Moreover, researchers still assume that in the absence of precipitation the scattering of UHF radiation and its absorption in the atmosphere can be neglected [1–3]. In other words, when conducting measurements and analyzing the results of a passive location at a frequency of 1.4 GHz, the atmosphere is considered absolutely transparent, which is completely untrue [2,4,6,14].

We also note that direct vertical measurements of the incident and reflected powers of the radiation flux (1)–(4) in time make it possible to study the evolution of the D and E layers of the ionosphere under various geophysical conditions. Accordingly, the change in the value $f(t)$, defined by expressions (8) and (11) is important directly for the problems of meteorology. Relations (1)–(4), (6) and (10)–(16), in turn, can be useful for reconstructing the parameters of a nonequilibrium two-temperature plasma (including the concentration of slow electrons ne and their temperature T_e), which can vary significantly during measurements. A clear demonstration of the changes in the plasma parameters of the D and E ionospheric layers with time is given in the work [23]. Therefore, it is necessary to attract additional information that can be obtained using GNSS systems for the correct interpretation of the results of the satellite measurements.

2.3. The Effect of Atmospheric Aerosols on the Propagation of Radio Waves

A not less important issue is related to the dynamics of the behavior of atmospheric factors $f_1(t)$ and $f_2(t)$ due to the reflection of radio waves at a frequency of 1.4 GHz, which depend on the

composition and charge of atmospheric aerosols. The key here is the problem of attenuation of the power flux of UHF radiation during its passage through charged aerosol layers in the atmosphere. It is well known that, when considering the propagation of radio waves, it is necessary to take into account the influence of not only atmospheric gases, but also aerosols of anthropogenic and natural origin. Although the weight concentration of substances in the aerosol state is low, their influence on the process of electromagnetic radiation propagation is significant due to the fact that aerosol particles can lead to separation of charges in the atmosphere and create significant negatively charged zones. This phenomenon causes the formation of atmospheric electric discharges.

The consideration of the kinetics of particle charging in the atmosphere is an extremely difficult task, which, however, must be solved to take into account distortions and losses of satellite radio signals. The process for charging the aerosol particles goes mainly by capturing the free electrons that result from ionization of carrier atmosphere. Of course, other heavier cosmic particles (including α -particles) can contribute to this process. Under ordinary conditions, several tens of charged pairs are formed in the troposphere. Free electrons interact with oxygen, and the resulting negative ions efficiently deposit on submicron particles that are always present in the air, even in the cleanest conditions. Positive ions then form heavy clusters in reactions with water molecules.

The complexity of considering the particle charging is associated with the fact that the mean free path of an ion is comparable to the Coulomb length, i.e., the distance at which the energy of thermal motion becomes comparable with the molecular mean free path. This means that it is impossible to apply the free molecular approximation, even for very small particle sizes (large Knudsen numbers). An effective and fairly simple solution to this problem is described in [24–30]. The diffusion limit was studied in [31], where the possible chemical interaction of ions with molecular impurities in the carrier gas was also taken into account.

Another important aspect is the need to take into account the effect of acid emissions on the radiation flux power of the D layer in the lower atmosphere, which is an independent task. Many physicochemical processes affecting the passage of a signal through the troposphere are currently studied in sufficient detail. Nevertheless, problems remain in the physical chemistry of the process that have not yet been adequately studied. First of all, these include the hydration of aerosol ions. As is known, it determines their mobility and affects the rate of chemical reactions, including diffusion processes, where the mobility of ions should also be considered together with the hydration shell. The latter also applies to the problem of the passage of incoherent microwave radiation through aerosol layers, where the processes occurring in the aerosols themselves remain especially significant [32–34].

3. Determination of Parameters of Nonequilibrium Plasma from IR Irradiation Spectra

The most promising method for monitoring the concentration n_e and the temperature T_e of slow electrons with energies below 10 eV in D and E ionospheric layers as the functions of time is to restore them by solving the inverse problem on the spectrum of far infrared radiation (in the wavelength range of 15–100 μm), as measured on a low-orbit satellite [7]. This imposes certain restrictions on IR sensors, which, along with high resolution, should have small dimensions and weight. The sensor used in [9] did not meet these conditions. A way out of this situation has been recently found after the emergence of metamaterials with unique optical properties associated with anomalous reflection and refraction [35,36], which stimulated the development of fundamentally new IR sensors.

Figure 2 shows the block diagram of such a sensor, where the filters are replaced by metasurfaces. The circuit is designed based on the performance requirements of the measuring device. Currently, Japan and the USA are actively involved in the creation of devices using such metasurfaces. Accordingly, the GRES program of the Japanese Agency for Science and Technology has already implemented the latest single-photon detectors in the wavelength range of 10–50 μm , which are GaAs/ALGaAs charge-sensitive transistors with an equivalent noise level of $8.3 \cdot 10^{-10}$ W/Hz and they are ready for serial production [37]. Moreover, the total weight of the equipment does not exceed 200 g. The following modification (with wavelengths up to 100 μm) is being developed at the University of Massachusetts

in the USA under the CLAREO program, which have the same characteristic parameters and are designed with the requirements for their reliable operation in both normal and cryogenic conditions, as well as vibration resistance when the satellite is in orbit [38].

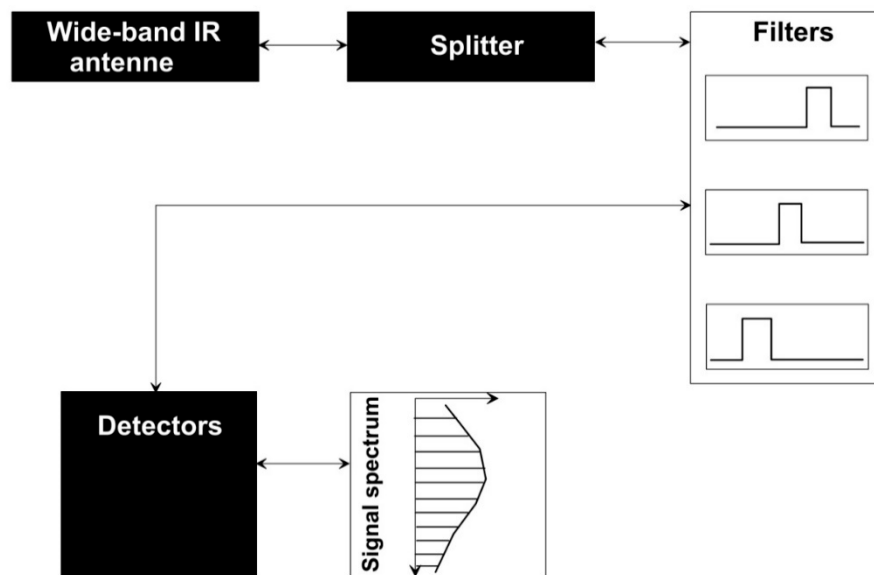


Figure 2. Block diagram of the sensor for measuring the spectrum of incoherent IR radiation.

4. The Problem of Calibration in Passive Remote Sensing

The calibration of measuring equipment (installed on a satellite or aircraft) is the next fundamental scientific and technical problem, allowing one to connect the sensors with determined physical parameters (humidity, structure and chemical composition, magnetic properties of a reflecting surface, etc.). Moreover, in contrast to direct ground-based measurements, satellites receive simultaneously both the reflected signal from the Earth's surface and the radiation from the uppermost atmosphere. Therefore, the calibration of the measured equipment and the restoration of the physical parameters of the surface should be based on a detailed analysis of the interactions of the initial radiation with the propagation medium and the Earth's surface.

The traditional method of satellite calibration is called vicarious and is as follows. The necessary relationships between the output signals of the sensors and the desired physical quantities are found by directly comparing the measured signals with the absolute standard of these quantities before launching the satellite, i.e., calibration is performed directly on the Earth [39]. Usually, a spectral window is used here with a central frequency of 1.413 GHz and a bandwidth of 27 MHz, which corresponds to cosmic radiation due to the lower forbidden transition in the hydrogen atom. The principal drawback of such a calibration is the complete disregard for variations in the parameters of the sensors over time due to the presence of the incoherent super background radiation of D and E layers of the ionosphere in a wide frequency range (including the frequency of 1.4 GHz, the intensity of which constantly varies with time). It is also necessary to take into account the influence of the above effects of attenuation of radiation intensity due to inhomogeneities of the lower atmosphere. To get out of this situation, it is advisable to switch to the two-frequency measurement method and take advantage of the fact that the microwave radiation intensity I_{MWR} is proportional to the square of the concentration of free electrons ($I_{MWR} \sim n_e^2$) at a frequency of $\nu_1 = 1.4$ GHz, and its first degree ($I_{MWR} \sim n_e$) at a frequency of $\nu_2 = 5.0$ GHz [3,14].

4.1. Two-Frequency Method of Passive Remote Sensing

In the case when the measurements on the Earth’s surface are not carried out [40], it is convenient to use relations (1)–(4) and expression (9). Assuming that the f value at these frequencies varies slightly, it is not difficult to show that the relative reflection coefficient is as follows (16):

$$\theta(H_s) = \frac{I_{\text{ref},1}^{(z\uparrow)}(H_E)}{I_{\text{ref},2}^{(z\uparrow)}(H_E)} = \frac{\Delta_1(H_s)}{\Delta_2(H_s)}. \tag{16}$$

Here, indices 1 and 2 denote the corresponding quantities for the frequencies $\nu_1 = 1.4$ GHz and $\nu_2 = 5.0$ GHz. Subsequently, the relative absorption coefficient is defined as (17)

$$\chi(H_E) = \frac{I_{\text{in},1}^{(z\downarrow)}(H_E) - I_{\text{ref},1}^{(z\uparrow)}(H_E)}{I_{\text{in},2}^{(z\downarrow)}(H_E) - I_{\text{ref},2}^{(z\uparrow)}(H_E)} \tag{5}$$

and takes the following form (18)

$$\chi(H_E) = \left(\frac{1 - k_{r,1}(H_E)}{1 - k_{r,2}(H_E)} \right) \frac{\bar{I}_{\text{tot},1}^{(z\downarrow)}(H_E)}{\bar{I}_{\text{tot},2}^{(z\downarrow)}(H_E)}, \tag{18}$$

where $k_{r,1}(H_E)$ is given by relation (10) and it is determined by the values of flux power $\bar{I}_{\text{tot},1}^{(z\downarrow)}(H_E)$ and $\bar{I}_{\text{tot},2}^{(z\downarrow)}(H_E)$ calculated using the “Rydberg” program. The simultaneous use of the base frequency $\nu_1 = 1.4$ GHz and additional second frequency $\nu_2 = 5.0$ GHz allows for us to reduce the problem to a one-parameter one, since the dependence of the quantities on the electron temperature T_e disappears and only the dependence on the electron concentration n_e remains.

4.2. The Role of IR Radiation Spectrum

The solution to the calibration problem of measuring equipment is impossible without monitoring the parameters of the two-temperature plasma in the E and D layers of the ionosphere. Therefore, the next important area of research is a detailed study of the characteristics of the IR radiation spectrum (where the main contribution is made by radiation transitions $\Delta n \geq 1$, where n is a principal quantum number of Rydberg state), which is directly related to the incoherent UHF radiation considered above [3]. Because the shape of the emission line of Rydberg states is very critical to the distribution of electron concentration and temperature inside these layers, measuring the IR spectrum on a satellite can serve as the basis for solving the inverse problem of restoring the dependence of the main plasma parameters and their height distribution on time. Reliable information on the shape of the IR spectrum will also make it possible to calculate using the «Rydberg» program [6,7,14], which is dependent on the height of the population of Rydberg states.

5. Conclusions

The main goal of our work was the explanation of a number of observed phenomena that, up to now, did not find a proper explanation. In our paper, we suggest, for the first time, a theoretically grounded principally new scheme of measurements. The scheme assumes that the radiation source exists below the satellite orbit and accounts for the fact that two types of radiation (direct and reflected) reach the satellite sensor. The separation of the respective fluxes is a serious problem that should be solved for correct interpretations of the measurements.

When conducting passive remote sensing of the Earth, it is necessary to have a method of calibration of measuring equipment. Attempts to circumvent this problem using the differential measurement method (using two antennas located up and down simultaneously) did not succeed due

to the specifics of incoherent UHF radiation, which is due to the fact that the radiation source is not point-like and it is spatially widely distributed in the low ionosphere. The next interfering factor is the mismatch of the viewing areas of the antennas used. To carry out the calibration of measuring equipment and measurements independent of time, it is necessary, at any time, to know the power of the radiation flux coming to the surface at frequencies of $\nu_1 = 1.4$ GHz and $\nu_2 = 5.0$ GHz.

Because the source of this radiation is Rydberg particles [1–3], the knowledge of the distribution function of their concentration in the emitting layer (80–110 km) will make it possible to determine the power of the incoming stream in real time. It is well known that Rydberg particles emit simultaneously in UHF and far IR range [3]. Therefore, it is most expedient to restore the distribution of their concentration using the IR spectrum measured on satellites in the wavelength range of 15–100 μm , which will additionally require complex mathematical signal processing [41,42]. Moreover, the sensors in the indicated range must be vibration-proof and operate in cryogenic conditions, which is a rather complicated scientific and technical task.

The complex self-consistent method that is presented in the paper combines the measured (with taking into account the absorption) and calculated using “Rydberg” program (without absorption) values. The intensities of incident and reflected radiations on the airship and on the Earth’s surface are measured. The intensities of incident radiation to the satellite, to the airship, and to the ground without taking into account the absorption are calculated. Altogether, these data allow one to determine the flux power attenuation in propagating the radiation from the D-layer to the airship, from the airship to the Earth’s surface, and the Earth’s surface reflection coefficient. It is important to note that the calculations and the measurements done separately from each other will not lead to the desired result.

Author Contributions: Conceptualization, G.V.G., M.I.M., A.A.L. and I.I.M.; Methodology, G.V.G., M.I.M., A.V.D. and M.G.G.; Software, S.O.A., Y.A.D. and M.G.G.; Validation, A.N.M.; Formal analysis, G.V.G., L.V.E., A.N.M. and M.G.G.; Writing—original draft preparation, G.V.G. and M.I.M.; Writing—review and editing, A.A.B., L.V.E., A.A.L., A.V.D. and M.G.G.; Visualization—M.I.M. and L.V.E.; Supervision—A.A.B.; Project administration—M.G.G. All authors have read and agreed to the published version of the manuscript.

Funding: This work was carried out in the framework of State Assignment of the Ministry of Science and Higher Education of the Russian Federation (project No. AAAA-A19-119010990034-5). The work of A.V. Dmitriev was supported by MOST (grant MOST No. 108-2111-M-008-035).

Conflicts of Interest: The authors declare no conflict of interest.

References

1. Golubkov, G.V.; Manzhelii, M.I.; Lushnikov, A.A. Radiochemical Physics of the Upper Earth’s Atmosphere. *Russ. J. Phys. Chem. B* **2014**, *8*, 604–611. [[CrossRef](#)]
2. Golubkov, G.V.; Manzhelii, M.I.; Berlin, A.A.; Lushnikov, A.A. Fundamentals of radio-chemical physics of the Earth’s atmosphere. *Russ. J. Phys. Chem. B* **2016**, *10*, 77–90. [[CrossRef](#)]
3. Kuverova, V.V.; Adamson, S.O.; Berlin, A.A.; Bychkov, V.L.; Dmitriev, A.V.; Dyakov, Y.A.; Eppelbaum, L.V.; Golubkov, G.V.; Lushnikov, A.A.; Manzhelii, M.I.; et al. Chemical physics of D and E layers of the ionosphere. *Adv. Space Res.* **2019**, *64*, 1876–1886. [[CrossRef](#)]
4. Golubkov, G.V.; Golubkov, M.G.; Manzhelii, M.I. Microwave and IR radiation of the upper atmosphere during periods of enhanced solar activity. *Dokl. Phys.* **2012**, *57*, 461–464. [[CrossRef](#)]
5. Su, S.-Y.; Tsai, L.-C.; Liu, C.H.; Nayak, C.; Caton, R.; Groves, K. Ionospheric Es layer scintillation characteristics studied with Hilbert-Huang transform. *Adv. Space Res.* **2019**, *64*, 2137–2144. [[CrossRef](#)]
6. Golubkov, G.V.; Manzhelii, M.I.; Golubkov, M.G. Microwave Radiation in the Upper Atmosphere of Earth During Strong Geomagnetic Disturbances. *Russ. J. Phys. Chem. B* **2012**, *6*, 112–127. [[CrossRef](#)]
7. Golubkov, G.V.; Golubkov, M.G.; Manzhelii, M.I. Additional background radiation of the atmosphere D layer within the frequency range from 0.8 to 6.0 GHz. *Dokl. Phys.* **2013**, *58*, 424–427. [[CrossRef](#)]
8. Avakyan, S.V. Physics of the solar-terrestrial coupling: Results, problems, and new approaches. *Geomagn. Aeron.* **2008**, *48*, 417–424. [[CrossRef](#)]

9. Mlynczak, M.G.; Johnson, D.G.; Latvakovski, H.; Jucks, K.; Watson, M.; Kratz, D.P.; Bingham, G.; Traub, V.A.; Wellard, S.J.; Hyde, C.R.; et al. First light from the far-infrared spectroscopy of the troposphere (FIRST) instrument. *Geophys. Res. Lett.* **2006**, *33*, L07704:1–L07704:4. [[CrossRef](#)]
10. Shklovsky, I.S. *The Problems of Modern Astrophysics*; Nauka: Moscow, Russia, 1988; p. 256.
11. Martynov, D.Y. *General Astronomy Course*; Fizmatlit: Moscow, Russia, 1988; p. 640.
12. Cooper, K. SETI: The water hole. *Astron. Now* **2010**, *4*, 1–6.
13. Golubkov, G.V.; Golubkov, M.G.; Manzhelii, M.I. Rydberg states in the D layer of the atmosphere and the GPS positioning errors. *Russ. J. Phys. Chem. B* **2014**, *8*, 103–115. [[CrossRef](#)]
14. Kerr, Y.H.; Waldteufel, P.; Wigneron, J.P.; Martinuzzi, J.; Font, J.; Berger, M. Soil moisture retrieval from space: The soil moisture and ocean salinity (SMOS) mission. *IEEE Trans. Geosci. Remote Sens.* **2001**, *39*, 1729–1735. [[CrossRef](#)]
15. Johnson, B.; Johnson, J. Sun in Radio Spectrum at 1.4 GHz. Available online: <https://www.thunderbolts.info/wp/2012/03/30/essential-guide-to-the-eu-chapter-11/sun-in-radio-spectrum-at-1-4-ghz/> (accessed on 18 June 2020).
16. Liljegren, J.C.; Lesht, B.M.; van Hove, T.; Rocken, C. A comparison of integrated water vapor from microwave radiometer, balloon-borne sounding system, and global positioning system. In Proceedings of the Ninth ARM Science Team Proceedings, San Antonio, TX, USA, 22–26 March 1999.
17. Le Vine, D.M.; Abraham, S. Faraday rotation correction for SMAP and soil moisture retrieval. *IEEE Trans. Geosci. Remote Sens.* **2018**, *56*, 665–668. [[CrossRef](#)]
18. Saleh, K.; Wigneron, J.P.; de Rosnay, P.; Calvet, J.C.; Escorihuela, M.J.; Kerr, Y.; Waldteufel, P. Impact of rain interception by vegetation and mulch on the L-band emission of natural grass. *Remote Sens. Environ.* **2006**, *101*, 127–139. [[CrossRef](#)]
19. Rudiger, C.; Walker, J.P.; Kerr, Y.H.; Mialon, A.; Merlin, O.; Kim, E.J. Validation of the level 1c and level 2 SMOS products with airborne and ground-based observations. In Proceedings of the 19th International Congress on Modelling and Simulation, Perth, Australia, 12–16 December 2011; pp. 2002–2008. Available online: <https://www.mssanz.org.au/modsim2011/E4/rudiger.pdf> (accessed on 18 June 2020).
20. Hallikainen, M.T.; Ulaby, F.T.; Dobson, M.C.; El-Rayes, M.A.; Wu, L.K. Microwave Dielectric Behavior of Wet Soil—Part I: Empirical Models and Experimental Observations. *IEEE Trans. Geosci. Remote Sens.* **1985**, *23*, 25–34. [[CrossRef](#)]
21. Dobson, M.C.; Ulaby, F.T.; Hallikainen, M.T.; El-Rayes, M.A. Microwave Dielectric Behavior of Wet Soil—Part II: Dielectric Mixing Models. *IEEE Trans. Geosci. Remote Sens.* **1985**, *23*, 35–45. [[CrossRef](#)]
22. Howell, J.R.; Menges, M.P.; Siegel, R. *Thermal Radiation Heat Transfer*; CRS Press: Boca Raton, FL, USA, 2015; p. 1016.
23. Afraimovich, E.L.; Astafieva, E.I.; Bergardt, O.I.; Demyanov, V.V.; Kondakova, T.N.; Lesyuta, O.S.; Shpynev, B.G. Mid-latitude amplitude scintillation of GPS signals and GPS failures at the auroral oval boundary. *Radiophys. Quantum Electron.* **2004**, *47*, 453–468. [[CrossRef](#)]
24. Lushnikov, A.A.; Kulmala, M. Charging of aerosol particles in the near free-molecule regime. *Eur. Phys. J. D At. Mol. Opt. Plasm. Phys.* **2004**, *29*, 345–355. [[CrossRef](#)]
25. Lushnikov, A.A.; Kulmala, M. Flux-matching theory of particle charging. *Phys. Rev. E* **2004**, *70*, 046413:1–046413:20. [[CrossRef](#)]
26. Lushnikov, A.A.; Kulmala, M. A kinetic theory of particle charging in the free-molecule regime. *J. Aerosol. Sci.* **2005**, *36*, 1069–1088. [[CrossRef](#)]
27. Lushnikov, A.A.; Zagaynov, V.A.; Lyubovtseva, Y.S. Formation of the aerosols in the Atmosphere. In *The Atmosphere and Ionosphere: DYNAMICS, Processes and Monitoring*; Bychkov, V.L., Golubkov, G.V., Nikitin, A.I., Eds.; Springer: New York, NY, USA, 2010; pp. 69–95. [[CrossRef](#)]
28. Lushnikov, A.A. Introduction to aerosols. In *Aerosols—Science and Technology*; Agranovski, I., Ed.; Wiley-VCH Verlag: Weinheim, Germany, 2010; pp. 1–41. [[CrossRef](#)]
29. Lushnikov, A.A. Nanoaerosols in the atmosphere. In *The Atmosphere and Ionosphere: Elementary Processes, Discharges and Plasmoids*; Bychkov, V.L., Golubkov, G.V., Nikitin, A.I., Eds.; Springer: New York, NY, USA, 2013; pp. 79–164. [[CrossRef](#)]
30. Elperin, T.; Fominykh, A.; Krasovitev, B.; Lushnikov, A. Isothermal absorption of soluble gases by atmospheric nanoaerosols. *Phys. Rev. E* **2013**, *87*, 012807:1–012807:8. [[CrossRef](#)] [[PubMed](#)]

31. Lushnikov, A.A.; Golubkov, G.V. Evaporation of a particle into chemically reactive carrier gas. *Russ. J. Phys. Chem. B* **2011**, *5*, 959–968. [[CrossRef](#)]
32. Kravitz, B.; Robock, A.; Oman, L.; Stenchikov, G.; Marquardt, A.B. Sulfuric acid deposition from stratospheric geoengineering with sulfate aerosols. *J. Geophys. Res. Atmos.* **2009**, *114*, D14109:1–D14109:7. [[CrossRef](#)]
33. Vasiliev, E.S.; Knyazev, V.D.; Savelieva, E.S.; Morozov, I.I. Kinetics and mechanism of the reaction of fluorine atoms with trifluoroacetic acid. *Chem. Phys. Lett.* **2011**, *512*, 172–177. [[CrossRef](#)]
34. Karpov, G.V.; Morozov, I.I.; Vasiliev, E.S.; Strokova, N.E.; Savilov, S.V.; Lunin, V.V. Hydration of negative ions of trichloroacetic acid in aqueous solutions. *Chem. Phys. Lett.* **2013**, *586*, 40–43. [[CrossRef](#)]
35. Cai, W.; Shalae, V. *Optical Metamaterials: Fundamentals and Applications*; Springer: New York, NY, USA, 2009; p. 200. [[CrossRef](#)]
36. Yu, N.; Genevet, P.; Kats, M.A.; Francesco, A.; Tietjenne, J.P.; Capasso, F.; Cabarro, Z. Light propagation with phase discontinuities: Generalized laws of reflection and refraction. *Science* **2011**, *334*, 333–337. [[CrossRef](#)]
37. Ueda, T.; Komiyama, S. Novel ultra-sensitive detectors in the 10–50 μm wavelength range. *Sensors* **2010**, *10*, 8411–8423. [[CrossRef](#)]
38. Cataldo, G. Development of Ultracompact High-Sensitivity, Space-Based Instrumentation for Far-Infrared and Submillimeter Astronomy. Ph.D. Thesis, Massachusetts Institute of Technology, Cambridge, MA, USA, 2015; p. 131.
39. Müller, R. Calibration and verification of remote sensing instruments and observations. *Remote Sens.* **2014**, *6*, 5692–5695. [[CrossRef](#)]
40. Sharkov, E.A. *Passive Microwave Remote Sensing of the Earth. Physical Foundations*; Springer: Berlin/Heidelberg, Germany, 2003; p. 613.
41. Eppelbaum, L.; Alperovich, L.; Zheludev, V.; Pechersky, A. Application of informational and wavelet approaches for integrated processing of geophysical data in complex environments. In Proceedings of the Symposium on the Application of Geophysics to Engineering and Environmental Problems, Charleston, South Carolina, 10–14 April 2011; pp. 461–497. [[CrossRef](#)]
42. Alperovich, L.; Eppelbaum, L.; Zheludev, V.; Dumoulin, J.; Soldovieri, F.; Proto, M.; Bavusi, M.; Loperte, A. A new combined wavelet methodology: Implementation to GPR and ERT data obtained in the Montagnole experiment. *J. Geophys. Eng.* **2011**, *10*, 025017:1–025017:17. [[CrossRef](#)]



© 2020 by the authors. Licensee MDPI, Basel, Switzerland. This article is an open access article distributed under the terms and conditions of the Creative Commons Attribution (CC BY) license (<http://creativecommons.org/licenses/by/4.0/>).